

Optical transmission of an atomic vapor in the mesoscopic regime

T. Peyrot, Y.R.P. Sortais, J.-J. Greffet, and A. Browaeys
*Laboratoire Charles Fabry, Institut d'Optique Graduate School,
CNRS, Université Paris-Saclay, F-91127 Palaiseau Cedex, France*

A. Sargsyan
Institute for Physical Research, National Academy of Sciences - Ashtarak 2, 0203, Armenia

J. Keaveney, I.G. Hughes, and C.S. Adams
Department of Physics, Rochester Building, Durham University, South Road, Durham DH1 3LE, United Kingdom

By measuring the transmission of near-resonant light through an atomic vapor confined in a nano-cell we demonstrate a mesoscopic optical response arising from the non-locality induced by the motion of atoms with a phase coherence length larger than the cell thickness. Whereas conventional dispersion theory – where the local atomic response is simply convolved by the Maxwell-Boltzmann velocity distribution – is unable to reproduce the measured spectra, a model including a non-local, size-dependent susceptibility is found to be in excellent agreement with the measurements. This result improves our understanding of light-matter interaction in the mesoscopic regime and has implications for applications where mesoscopic effects may degrade or enhance the performance of miniaturized atomic sensors.

One important characteristic of mesoscopic systems is the fact that their properties are not ruled by local quantities. The mesoscopic regime arises when the size of the system becomes smaller than a distance ξ characterizing the non-local response of the medium to an excitation. Non-locality is thus a prerequisite to the observation of mesoscopic behaviors. For instance, the concept of local conductivity fails to describe the transport of electrons or phonons when the distance over which the phase of the carriers is lost exceeds the size of the system, as is the case in nano-wires [1, 2]. In these systems the electrical potential (or the temperature) is undefined and one uses instead a global conductance. Also, non-local effects are at the origin of the low temperature anomalous conductivity of a metal at frequencies ranging from GHz to infrared [3], as the skin depth over which the field varies near a surface is smaller than the mean-free path of the electrons in the metal [4, 5].

In optics, non-locality is often observed in *non-linear* bulk media [6, 7], in particular in the presence of long-range interactions between particles [8]. In contrast, manifestations of non-local optical properties in *linear* media are scarce. They have been observed for molecules near metallic surfaces [9, 10] and the mesoscopic regime was reached with nano-particles for which the electron mean-free path is on the order of the particle size [11, 12]. Also, the *selective reflection* at the interface between a glass and a bulk atomic vapor [13–15] was interpreted as an indirect evidence of non-locality originating from the motion of the atoms and their transient response following a collision with the glass surface [16–20]. Confining the vapor in nano-cells, i.e. cells with sub-wavelength thickness, the non-locality should give rise to a mesoscopic response, as the system size is now on the order of the phase coherence length ξ , as explained below. These nano-cells are considered as potential atomic sensors [20, 21] and ideal media to explore atom-light [22] and atom-surface interactions [23]. It is therefore important to understand how

the mesoscopic response may affect the precision of these sensors. So far, the interplay between non-locality and system-finite size have been very little studied in nano-cells [24] with no comparison between experiment and theory. In particular, the question remains whether the concept of susceptibility holds in this mesoscopic system.

Here, we systematically study the mesoscopic optical response of a hot vapor of cesium confined in a nano-cell. We measure the transmission spectra for various cell thicknesses and observe that they cannot be reproduced by a model assuming a local susceptibility. We develop a theoretical model where we calculate explicitly the mesoscopic optical response of the vapor accounting for the non-locality arising from the motion of the atoms and for the breaking of translational invariance due to the presence of interfaces. In particular, our model defines clearly the parameter regime (velocity, density, and size of the system) where non-locality dominates in atomic vapors, identifies the role of the system finite-size and reproduces remarkably well the observed spectra.

In any *homogeneous* medium, the relation between the polarization vector and the electric field at a frequency ω is given by (one-dimensional model) [25]:

$$P(z, \omega) = \int_{-\infty}^{+\infty} \epsilon_0 \chi(z - z', \omega) E(z') dz', \quad (1)$$

where the susceptibility $\chi(z - z', \omega)$ describes the spatial response of the medium and typically decays over a distance ξ , the so-called range of non-locality. In an atomic vapor, the non-locality comes from the motion of the atoms and ξ is equal to their phase coherence length, i.e. the distance travelled by the atoms before the phase of the light excitation imprinted on them is lost (due to collisions with other particles or to radiative decay): $\xi = v/\Gamma_t$ with v the atom velocity and Γ_t the total homogeneous linewidth [16, 17, 19]. Typically, in a room temperature vapor of alkali, $\xi \approx 3 \mu\text{m}$. In a nano-cell,

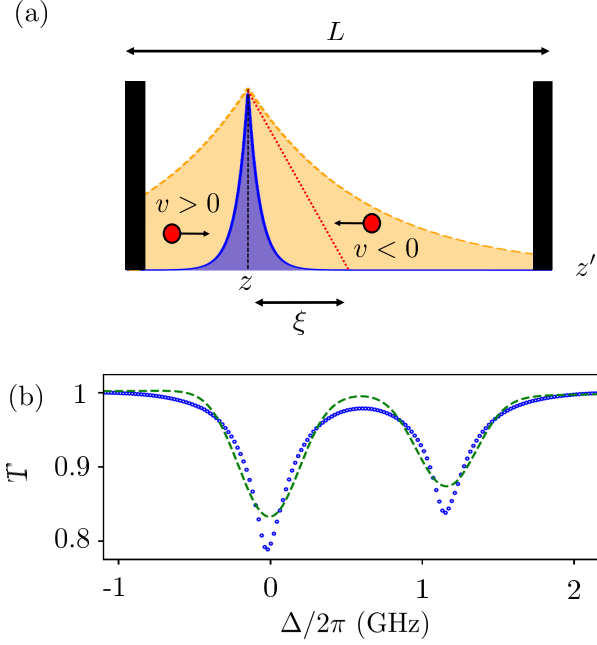


FIG. 1: (a) Illustration of the non-local response in presence of an interface in a slab of thickness L . Orange fill: non local response χ for $\xi \sim L$. Blue fill: local response χ for $\xi \ll L$. (b) Blue line: experimental transmission spectrum for $L = 420$ nm and $\Theta \approx 170^\circ\text{C}$ as a function of the laser detuning Δ with respect to the transition $F = 4$ to $F' = 3$. The data are binned 10 times by steps of 2 MHz. The lines correspond respectively to the Cs D1 hyperfine transitions $F = 4$ to $F' = 3$ (left), and $F = 4$ to $F' = 4$ (right). Dashed green line: fit by the first local model.

the presence of the walls separated by L breaks the translational invariance (see Fig. 1(a)) and the mesoscopic regime is achieved as soon as $\xi \gtrsim L$. In this regime, the non-local relation between P and E (Eq. (1)) also depends on L and the concept of size-independent susceptibility collapses, as is also the case in nano-photonic devices [9, 10, 26–28].

To observe the mesoscopic optical response resulting from non-locality, we confine a Cs vapor in a wedged sapphire nano-cell of refractive index $n_s = 1.76$, the thickness of which varies from 30 nm to $2 \mu\text{m}$ [29, 30]. The cell is mounted in a home-made oven that allows differential heating between the reservoir and the windows. The reservoir temperature Θ is monitored by a thermocouple and is related to the atomic density N in the cell via the vapor pressure. An external-cavity diode laser is scanned at 10 Hz around the Cs D1 line at $\lambda = 894$ nm (natural linewidth $\Gamma = 2\pi \times 4.6$ MHz) and we use a 7 cm spectroscopic cell as a reference for frequency calibration. The 700 nW laser beam is focused with a waist of $\sim 40 \mu\text{m}$ and scanned along the wedge to explore various thicknesses L of the atomic slab. We use the back reflections on the nano-cell to determine L using an interferometric method [31]. Finally, the transmitted light is collected on a photodiode.

When the temperature of the vapor increases, so do the den-

sity and the homogeneous linewidth due to collisional dipole-dipole interactions. For $\Theta \geq 250^\circ\text{C}$, we observe linewidths as large as $\Gamma_t = 2\pi \times 1$ GHz leading to $\xi < L$, thus restoring locality [32]. To avoid this situation, we set the temperature of the vapor to a lower value ($\Theta \approx 170^\circ\text{C}$) to keep the expected homogeneous linewidth $\Gamma_t \approx 2\pi \times 60$ MHz [33] such that $\xi > 5L$. Operating at a lower temperature would make the mesoscopic response stronger, at the expense of a much lower absorption, hence reducing the signal-to-noise ratio. The choice of the temperature thus results from a compromise. We present in Fig. 1(c) an example of a transmission spectrum, normalized to the value of the signal far from the atomic resonances, for a thickness of the slab $L = 420$ nm. The lineshape appears more complicated than a sum of Gaussian or Lorentzian functions.

In an attempt to model the transmitted spectra, we first use the dispersion theory relying on a description of the vapor (density N) by a *local* susceptibility χ [34]. Specifically, we calculate χ by summing the contributions of all Doppler-broadened hyperfine transitions of the Cs D1 line at frequencies $\omega_{FF'}$ [35], assuming a normalized Maxwell-Boltzmann velocity distribution $M_v(v)$ along the laser direction of propagation (d is the dipole moment of the strongest transition, $C_{FF'}$ the Clebsch-Gordan coefficients):

$$\chi(\omega) = \frac{Nd^2}{\hbar\epsilon_0} \sum_{F,F'} C_{FF'}^2 \int_{-\infty}^{\infty} \frac{iM_v(v)}{\Gamma_t - 2i(\Delta_{FF'} - k_1v)} dv. \quad (2)$$

Here, $\Delta_{FF'} = \omega - \omega_{FF'} - \Delta_p$ and $\Gamma_t = \Gamma + \Gamma_p$, where we have introduced Δ_p and Γ_p a shift and a broadening characterizing the medium, which originates from the collisional dipole-dipole interactions and the atom-surface interactions [30]. The refractive index is then $n(\omega) = \sqrt{1 + \chi(\omega)}$. We account for the multiple reflections inside the cavity formed by the two sapphire plates (index n_s) surrounding the vapor using the transmission function:

$$t(\omega) = \frac{4n_s n \exp[i(n - n_s)k_1L]}{(n_s + n)^2 - (n_s - n)^2 \exp[2in k_1L]}. \quad (3)$$

Finally, we calculate the normalized transmission $T(\omega) = |t[n(\omega)]/t[n = 1]|^2$. The result of this first model is shown in Fig. 1(c), for which we have adjusted the values of N , Δ_p and Γ_p to best fit the data. Strikingly, it does not agree with the data: the experimental linewidth appears narrower than the calculated Doppler broadened width. This is a signature of the coherent Dicke narrowing already observed by many authors [24, 36–38]. In nano-cells, this emphasizes the failure of the conventional dispersion theory, which assumes a local susceptibility of the atomic gas and a Maxwell-Boltzmann velocity distribution.

In a second model, we introduce the effect of the cell walls in the simplest possible way: we assume that mainly the atoms flying parallel to the walls contribute to the signal, all the others colliding too rapidly with the walls to participate. We therefore take for the velocity distribution $M_v(v) = \delta(v)$ in Eq. (2) [39], to account phenomenologically for the velocity

selection. We fit the data letting as before N , Δ_P and Γ_P free to evolve. The result, shown in Fig. 2 for $L = 360$ nm, is in much better agreement with the data. Nonetheless, the residuals reveal that the model fails to reproduce the narrow feature near resonance, characteristic of the contribution from the slow atoms [15].

Finally, inspired by previous works [19, 40, 41], we derive a third, intrinsically non-local model that accounts both for the explicit k -dependence of the susceptibility and the collisions of the atoms with the surfaces of the nano-cell. To do so we first calculate the response function of the atomic medium assuming it is homogeneous and then we account for the influence of the surfaces [10]. The susceptibility in the (k, ω) space of an homogeneous gas of atoms with a velocity v is given, for a specific transition, by [42]:

$$\chi_{FF'}(k, \omega, v) = i \frac{d^2 C_{FF'}^2}{\hbar \epsilon_0} \frac{NM_v(v)}{\Gamma_t - 2i(\Delta_{FF'} - kv)}. \quad (4)$$

The k -dependence resulting from the Doppler effect is at the origin of the non-locality and leads to spatial dispersion [25]. Note that this non-locality is not specific to nano-cells, but appears in any atomic vapor. An inverse Fourier transform yields:

$$\chi_{FF'}(z - z', \omega, v) = iNM_v(v) \frac{d^2 C_{FF'}^2}{\hbar \epsilon_0 |v|} e^{(-\frac{\Gamma_t}{2} + i\Delta_{FF'}) \frac{z-z'}{v}} \quad (5)$$

for $(z - z')/v > 0$ and $\chi_{FF'}(z - z', \omega, v) = 0$ for $(z - z')/v < 0$, as required by causality. We recover the above-mentioned decay length $\xi = |v|/\Gamma_t$. As for the influence of the surfaces, we assume quenching collisions with the cell walls [16], i.e. the phases of the atomic coherences are reset upon collisions. Velocity classes $\pm v$ become independent and the presence of the walls therefore breaks the translational invariance in the medium [43]. We express this fact by multiplying $\chi_{FF'}(z - z', \omega, v)$ by a top-hat function ($\Pi_0^L(z') = 1$ for $0 < z' < L$ and is null elsewhere). When $\xi \gtrsim L$, the non-local response of the medium depends on the size L of the entire system, and is not characteristic of the medium only (see Fig. 1(b)). Finally, the response of the system is obtained by summing over all the atomic transitions: $\chi_L(z, z', \omega, v) = \sum_{F, F'} \Pi_0^L(z') \times \chi_{FF'}(z - z', \omega, v)$.

To calculate the field transmitted through the cell filled with the vapor, we also consider the multiple reflections inside the cavity formed by the sapphire windows. The transmitted field E_t is the superposition of the field transmitted by the empty cavity E_{t0} , and of the fields E_{t+} and E_{t-} initially scattered by the atoms in the forward and backward directions and that have undergone multiple reflections before being transmitted. The field transmitted by the empty cavity is $E_{t0} = t_1 t_2 / (1 - r_2^2 e^{2ik_1 L}) E_0 e^{ik_1 z}$ with $t_1 = 2n_s / (1 + n_s)$, $t_2 = 2 / (1 + n_s)$, $r_2 = (1 - n_s) / (1 + n_s)$ and $E_0 e^{ik_1 z}$ the incident field. The fields E_{t+} and E_{t-} are related to the polarization vector $P(z, \omega)$ inside the medium by [42]:

$$E_{t\pm}(z) = \frac{t_2}{1 - r_2^2 e^{2ik_1 L}} \frac{ik_1}{2\epsilon_0} \int_0^L dz' P(z', \omega) e^{ik_1(z \mp z')}, \quad (6)$$

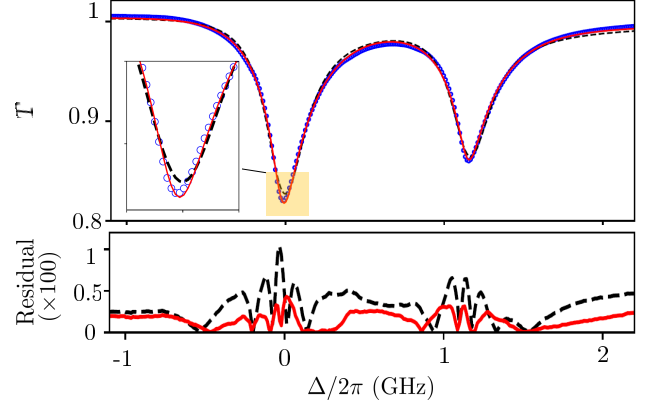


FIG. 2: Top panel. Blue dots: experimental transmission spectrum for $\Theta = 170^\circ\text{C}$ and $L = 360$ nm binned as in Fig. 1(c). Black dot-dashed line: fit by the second model. Red dashed line: fit by the third model (see text). Inset: zoom near resonance. Low panel: absolute value of the residuals for both fits.

where the polarization inside the medium is linked to the *total* cavity field $E(z)$ by the expression generalizing Eq. (1):

$$P(z', \omega) = \int_{-\infty}^{\infty} dz'' \int_{-\infty}^{\infty} dv \epsilon_0 \chi_L(z', z'', \omega, v) E(z''). \quad (7)$$

The integrals can be calculated [42], assuming the atomic medium to be dilute and thin enough so that the cavity field is approximately the one inside the empty cavity (Born approximation [44]): $E(z'') \approx t_1 / (1 - r_2^2 e^{2ik_1 L}) E_0 [e^{ik_1 z''} + r_2 e^{ik_1(2L - z'')}]$. Under this assumption, and taking a Maxwell velocity distribution, we compute them numerically to extract the normalized transmission $T(\omega) = |E_t/E_{t0}|^2$. After abandoning the description of the system by a size-independent response function, the transmission is now the global observable characterizing the optical response in our mesoscopic regime. Our approach starting from the non-local response function agrees with the formulae obtained in Ref. [41] under the same assumption, i.e. for low absorption.

The fit of the data by the third model is presented in Fig. 2 for the best found parameters N , Δ_P and Γ_P . The agreement is excellent. In particular, the narrow feature near resonance is reproduced accurately: despite the fact that we keep the full Maxwell velocity distribution, the velocity selection, imposed in the second phenomenological model and at the origin of the narrowing, is an automatic consequence of the third, non-local model. To further test the two last models, we also plot in Figs. 3(a,b) the value T_{\min} of the minimum of the transmission for the hyperfine transition from $F = 4$ to $F' = 3$ as a function of the cell thickness. We observe that both models are in good agreement with the data although the third model fits better around $L \approx \lambda/2$ [45]. Also, $T_{\min}(L)$ does not decay exponentially as the Beer-Lambert law would predict [34]. This is expected for two reasons. Firstly, the atoms being in a cavity, the transmitted field amplitude is not given by the Beer-Lambert law but by Eq. (3): a $\lambda/2$ -periodic oscil-

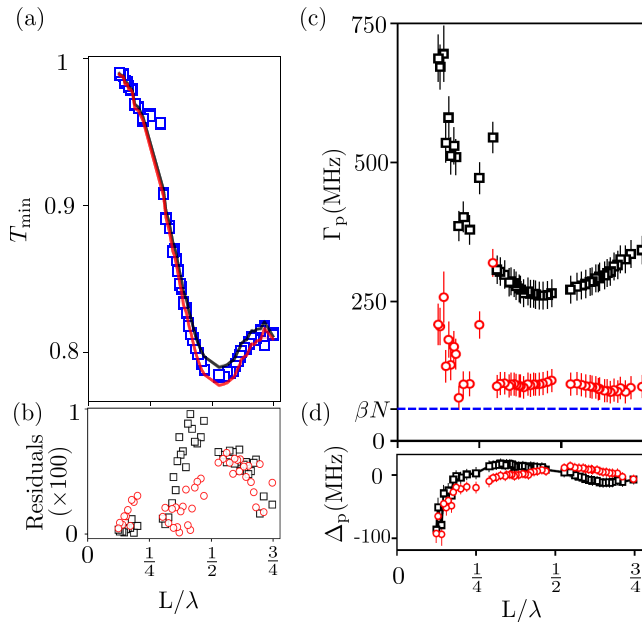


FIG. 3: (a) Minimum of transmission T_{\min} for the transition from $F = 4$ to $F' = 3$ against the cell thickness L . Blue squares: experimental data. Black and red lines: values deduced from the fit of the spectra using the second and third models, respectively. Error bars are smaller than markers. (b) Absolute value of the residuals for the second (black) and third (red) models. (c) (resp. d): broadening parameter Γ_p (resp. shift parameter Δ_p) obtained from the fit of the spectra using the second model (black squares) and third model (red circles). Error bars are the quadratic sum of statistic and fit errors. Blue dotted line: collisional broadening prediction [33].

lation, originating from the multiple reflections in the cavity, modulates the exponential decay. Secondly, even without the cavity, the field inside the vapor cannot be exponential due to the non-local character of the medium [16], which leads to a λ -periodic oscillation [42].

Even though the residuals in Fig. 2 could discriminate between the second phenomenological and third non-local models [46], the values of Δ_p and Γ_p returned by the fit indicate clearly that only the third model is correct, as we now discuss. Both parameters characterize the bulk properties of the vapor and the van der Waals interactions between the atoms and the surfaces. They depend *a priori* on the density N (constant at a given temperature of the vapor) and the cell thickness L . The L -dependence comes only from the atom-surface interaction, as for small L the fraction of atoms close to the surface is larger than for large L . For Cs, the theoretical atom-sapphire interaction coefficient C_3 is around a few $\text{kHz} \cdot \mu\text{m}^3$ [47, 48]: in the range $\lambda/4 \leq L \leq \lambda$ the influence of the surface on Γ_p and Δ_p is therefore expected to be smaller than 10 MHz and thus negligible. Importantly, the cavity effects are already taken into account in both models through the multiple reflections and therefore should not contribute to Γ_p and Δ_p [49]. For a fitting model to make sense, it should therefore return values of Γ_p and Δ_p independent of L . Figure 3(c) shows the

values of Γ_p returned by the fit for the two last models as a function of L . Only the third model is able to return a value independent of L for $L \geq 200$ nm. At smaller distances, Γ_p increases due to the atom-surface interaction [42]. Furthermore, for $L \geq 200$ nm, Γ_p is in reasonable agreement with the expected broadening βN due to collisional dipole-dipole interactions at the density corresponding to $\Theta \approx 170^\circ\text{C}$ [33]. The second, phenomenological model, by contrast, yields a strong dependence of Γ_p with L , which is not acceptable based on the arguments presented above. As a consequence the only model, which features both a good agreement with the data and a consistent interpretation of its fitting parameters, is the third one. Figure 3(d) presents the fitted Δ_p against L : the difference between the two models is less striking. Both feature the influence of the attractive atom-surface interaction at small thickness.

The situation studied in this work, of an atomic vapor where the phase coherence length exceeds the dimension of the system, is widely met in miniaturized atomic sensors. We have shown that the propagation of light through nano-cells cannot be described by any local property, and even the concept of non-local system-size-independent susceptibility collapses. The optical response of mesoscopic systems is now understood globally using a transmission factor. This situation is reminiscent of the electrical conduction in the mesoscopic regime where the concept of local conductivity is no longer valid and a global conductance has to be introduced. Our model makes explicit the role of non-locality and its dependence with the system size, and agrees with experimental data for extinctions as large as 20%. To our knowledge the agreement presented here between theory and experiment is unprecedented in both atomic hot and cold dense atomic vapors altogether [50]. Importantly, it allows the extraction of meaningful quantities such as energy shift and linewidth, hence providing a theoretical framework for characterizing future atomic sensors.

We thank D. Sarkisyan, G. Dutier, A. Laliotis and D. Bloch for discussions. T. Peyrot is supported by the DGA-DSTL fellowship 2015600028. We also acknowledge financial support from CNRS, EPSRC (grant EP/R002061/1) and Durham University. The data presented in this paper will be available later on.

-
- [1] N. Agraït, A.L. Yeyatib and J.M. van Ruitenbeek, Quantum properties of atomic-sized conductors, *Phys. Rep.* **377**, 81 (2003).
 - [2] K. Schwab, E.A. Henriksen, J.M. Worlock and M.L. Roukes, Measurement of the quantum of thermal conductance, *Nature* **404**, 974 (2000).
 - [3] A.B. Pippard, The surface impedance of superconductors and normal metals at high frequencies II. The anomalous skin effect in normal metals, *Proc. Roy. Soc. A* **191**, 385 (1947).
 - [4] F. Wooten, Optical properties of solids, Academic Press, New York (1972).

- [5] P.W. Gilbert, The anomalous skin effect and the optical properties of metals, *J. Phys. F* **12**, 1845 (1982).
- [6] R.W. Boyd, Non-Linear Optics, 3rd Ed., Academic press.
- [7] C. Rotschild, B. Alfassi, O. Cohen and M. Segev, Long-range interactions between optical solitons, *Nat. Phys.* **2**, 769 (2006)
- [8] H. Busche, P. Huillery, S.W. Ball, T. Ilieva, M.P.A. Jones and C.S. Adams, Contactless nonlinear optics mediated by long-range Rydberg interactions, *Nat. Phys.* **13**, 655 (2017)
- [9] C.F. Eagen, W.H. Weber, S.L. McCarthy and R.W. Threhune, Time-dependent decay of surface-plasmon-coupled molecular fluorescence, *Chem. Phys. Lett.* **75**, 274 (1980).
- [10] G.W. Ford and W.H. Weber, Electromagnetic interactions of molecules with metal surfaces, *Phys. Rep.* **113**, 195 (1984).
- [11] U. Kreibig and L. Genzel, Optical absorption of small metallic particles, *Surf. Science* **156**, 678 (1985)
- [12] Ch. Voisin, N. Del Fatti, D. Christofilos and F. Vallée, Ultrafast electron dynamics and optical nonlinearities in metal nanoparticles, *J. Phys. Chem. B* **105**, 2264 (2001).
- [13] J.L. Cojan, Contribution à l'étude de la réflexion sélective sur les vapeurs de mercure de la radiation de résonance du mercure, *Ann. Phys* **9**, 385 (1954).
- [14] A.L.J. Burgmans, M.F.H. Schuurmans and B. Bölger, Transient behavior of optically excited vapor atoms near a solid interface as observed in evanescent wave emission, *Phys. Rev. A* **16**, 5 (1977).
- [15] S. Briaudeau, S. Saltiel, G. Nienhuis, D. Bloch and M. Ducloy, Coherent Doppler narrowing in a thin vapor cell: Observation of the Dicke regime in the optical domain, *Phys. Rev. A* **57**, 5 (1998).
- [16] M.F.H. Schuurmans, Spectral narrowing of selective reflection, *Journal de Physique* **37**, 469 (1976).
- [17] G. Nienhuis, F. Schuller and M. Ducloy, Nonlinear selective reflection from an atomic vapor at arbitrary incidence angle, *Phys. Rev. A* **38**, 5197 (1988).
- [18] T.A. Vartanyan and F. Träger, Line shape of resonances recorded in selective reflection: influence of an antireflection coating, *Opt. Comm.* **110**, 315 (1994).
- [19] T.A. Vartanyan and D.L. Lin, Enhanced selective reflection from a thin layer of a dilute gaseous medium, *Phys. Rev. A* **51**, 1959 (1995).
- [20] R. Ritter, N. Gruhler, H. Dobbertin, H. Kübler, S. Scheel, W. Pernice, T. Pfau and R. Löw, Coupling thermal atomic vapor to slot waveguides, *Phys. Rev. X* **8**, 021032 (2018).
- [21] S. Knappe, P.D.D. Schwindt, V. Shah, L. Hollberg, J. Kitching, L. Liew and J. Moreland, A chip-scale atomic clock based on ^{87}Rb with improved frequency stability, *Opt. Exp.* **13**, 1249 (2005).
- [22] J. Keaveney, I.G. Hughes, A. Sargsyan, D. Sarkisyan and C.S. Adams, Refraction and superluminal propagation in a gaseous nanolayer, *Phys. Rev. Lett.* **109**, 233001 (2012).
- [23] A. Sargsyan, A. Papoyan, I.G. Hughes, C.S. Adams, and D. Sarkisyan, Selective reflection from an Rb layer with a thickness below $\lambda/12$ and applications, *Opt. Lett.* **42**, 1476 (2017).
- [24] G. Dutier and M. Ducloy, Collapse and revival of a Dicke-type coherent narrowing in a sub-micron thick vapor cell transmission spectroscopy, *Europhys. Lett.* **63**, 35 (2003).
- [25] L.D. Landau, L.P. Pitaevskii and E.M. Lifshitz, Electrodynamics of continuous media, Second Edition, Pergamon Press.
- [26] G.H. Cocoletzi and W.L. Mochán, Excitons: from excitations at surfaces to confinement in nanostructures, *Surf. Sc. Rep.* **57**, 1 (2005).
- [27] R.J. Churchill and T.G. Philbin, Electromagnetic reflection, transmission, and energy density at boundaries of nonlocal media, *Phys. Rev. B* **94**, 235422 (2016).
- [28] C. Tserkezis, N. A. Mortensen, and M. Wubs, How nonlocal damping reduces plasmon-enhanced fluorescence in ultranarrow gaps, *Phys. Rev. B* **96**, 085413 (2017).
- [29] D. Sarkisyan, D. Bloch, A. Papoyan *et. al*, Sub-Doppler spectroscopy by sub-micron thin Cs vapor layer, *Opt. Commun.* **200**, 201 (2001)
- [30] T. Peyrot, Y.R.P. Sortais, A. Browaeys, A. Sargsyan, D. Sarkisyan, J. Keaveney, I.G. Hughes and C.S. Adams, The collective Lamb Shift of a nanoscale atomic vapor layer within a sapphire cavity, *Phys. Rev. Lett.* **120**, 243401 (2018).
- [31] E. Jahier, J. Guéna, P. Jacquier, *et. al*, Temperature-tunable sapphire windows for reflection loss-free operation of vapor cells, *Appl. Phys. B* **71**, 561 (2000).
- [32] We used this possibility in our measurement of the collective Lamb shift in a dense vapor [30].
- [33] L. Weller, R.J. Bettles, P. Siddons, C.S. Adams and I.G. Hughes, Absolute absorption on the rubidium D1 line including resonant dipole-dipole interactions, *J. Phys. B* **44**, 195006 (2011).
- [34] C. S. Adams and I. G. Hughes Optics f2f, *Oxford University Press* (2019).
- [35] M.A. Zentile, J. Keaveney, L. Weller, D.J. Whiting, C.S. Adams and I.G. Hughes, ElecSus: A program to calculate the electric susceptibility of an atomic ensemble, *Comp. Phys. Comm.* **189**, 162 (2015).
- [36] R. Dicke, The effect of collisions upon the Doppler width of spectral lines, *Phys. Rev.* **89**, 472 (1953).
- [37] R.H. Romer and R. Dicke, New technique for high-resolution microwave spectroscopy, *Phys. Rev.* **99**, 532 (1955).
- [38] A. Sargsyan, Y. Pashayan-Leroy, C. Leroy *et. al*, Collapse and revival of a Dicke-type coherent narrowing in potassium vapor confined in a nanometric thin cell, *J. Phys. B* **49**, 075001 (2016).
- [39] We also consider in the Supplemental Material [42] the case of a bimodal distribution. The main conclusions of the paper are unchanged, but the price to pay is the introduction of two extra fitting parameters.
- [40] B. Zambon, G. Nienhuis, Reflection and transmission of light by thin vapor layers, *Opt. Comm.* **143** 308 (1997).
- [41] G. Dutier and M. Ducloy, Revisiting optical spectroscopy in a thin vapor cell: mixing of reflection and transmission as a Fabry Perot microcavity effect, *J. Opt. Soc. Am. B* **20**, 793 (2003).
- [42] See Supplemental Material.
- [43] This is in contrast to the case of elastic collisions at the wall [42].
- [44] R. Carminati and J.-J. Greffet, Influence of dielectric contrast and topography on the near field scattered by an inhomogeneous surface, *J. Opt. Soc. Am. A* **12**, 2716 (2003).
- [45] The odd behavior of the data around $L \simeq \lambda/4$, already pointed out in J. Keaveney *et al.* *Phys. Rev. Lett.* **108**, 173601 (2012) in a different context, is not understood and will be the subject of future investigations.
- [46] I.G. Hughes and T.P.A. Hase, Measurements and their Uncertainties: A Practical Guide to Modern Error Analysis (OUP, Oxford, 2010).
- [47] K.A. Whittaker, J. Keaveney, I.G. Hughes, A. Sargsyan, D. Sarkisyan and C.S. Adams, Optical response of gas-phase atoms at less than $\lambda/80$ from a dielectric surface, *Phys. Rev. Lett.* **112**, 253201 (2014).
- [48] D. Bloch and M. Ducloy, Atom-wall interaction, *Adv. Mol. Phys.* **50**, 91 (2005).
- [49] For the dilute vapor used here, the residual oscillatory dependence of Δ_p with L observed in [30] has an amplitude lower than 10 MHz, and is therefore negligible.
- [50] S. Jennewein, L. Brossard, Y.R.P. Sortais, A. Browaeys,

P. Cheinet, J. Robert and P. Pillet, Coherent scattering of near-resonant light by a dense, microscopic cloud of cold two-level atoms: Experiment versus theory, [Phys. Rev. A **97**, 053816](#) (2018).

Supplemental Material: Optical transmission of an atomic vapor in the mesoscopic regime

T. Peyrot, Y.R.P. Sortais, J.-J. Greffet, and A. Browaeys
*Laboratoire Charles Fabry, Institut d'Optique Graduate School,
CNRS, Université Paris-Saclay, F-91127 Palaiseau Cedex, France*

A. Sargsyan
Institute for Physical Research, National Academy of Sciences - Ashtarak 2, 0203, Armenia

J. Keaveney, I.G. Hughes, and C.S. Adams
*Department of Physics, Rochester Building, Durham University,
South Road, Durham DH1 3LE, United Kingdom*

Here, we first derive the equations of the third (non-local) model of the main text, starting with the expression of the non-local susceptibility (Eq. (5)). Then, we derive the expression of the optical field transmitted through a thin layer of atomic gas, first in vacuum, and then accounting for the presence of glass interfaces. In Section II, we show that using a bimodal velocity distribution in the second model of the main text cannot reproduce consistently the data either. In Section III we give more details about the deviation of the transmission coefficient from the Beer-Lambert law. Finally, we analyze in more details the thickness dependence of the parameter Γ_p extracted from the fit of the data by the local model.

I. DERIVATION OF THE NON-LOCAL MODEL

In this first Section, we derive the expression of the transmission through the atomic slab, including the cavity effect from the sapphire plates of the nanocell, making explicit the origin of the non-locality.

A. The non-local susceptibility

We start by deriving the expression of the non-local susceptibility $\chi(z, z', \omega, v)$ of the ensemble of atoms for a velocity class v and at frequency ω . As explained in the main text, the presence of the cell walls makes it a challenging task in general. To simplify the situation, we will use the following procedure:

1. We will treat the vapor as if it was homogeneous (i.e. in the absence of confining walls). In this case, the susceptibility depends only on the difference: $\chi(z, z', \omega, v) = \chi(z - z', \omega, v)$.
2. We will treat the effect of the surfaces separately. This will be done by assuming quenching collisions at the cell walls, i.e. the atomic coherence will be lost during these collisions [1] and reset to zero. In this way, there will not exist any relation between the coherence of atoms moving at $+v$ or $-v$, contrarily to what would happen if the collisions with the walls were elastic.

To derive the susceptibility for an homogeneous vapour, we first consider a given atomic transition between ground and excited states F and F' (frequency $\omega_{FF'}$, and total homogeneous linewidth Γ_t) described by a coherence ρ_{21} and a dipole matrix element $d_{FF'} = C_{FF'} d$ ($C_{FF'}$ is the Clebsch Gordan coefficient normalized to the strongest transition with dipole moment d). We write the field and polarization in the vapor in the form: $E(z, t) = \frac{1}{2} (E(z)e^{-i\omega t} + E^*(z)e^{i\omega t})$ and $P(z, t) = \frac{1}{2} (P(z)e^{-i\omega t} + P^*(z)e^{i\omega t})$. We introduce the coherence field $\rho_{21}(z, t, v)$ at position z in the slab for the velocity class v . In the low intensity limit (i.e. neglecting populations in the excited state), the Maxwell-Bloch equation for the coherence is [2]:

$$\frac{d\rho_{21}(z, t, v)}{dt} = -i\omega_{FF'}\rho_{21}(z, t, v) + iC_{FF'}\frac{dE(z, t)}{\hbar} - \frac{\Gamma_t}{2}\rho_{21}(z, t, v). \quad (1)$$

Using the convective derivative $d/dt = \partial/\partial t + v\partial/\partial z$, we get:

$$\frac{\partial\rho_{21}(z, t, v)}{\partial t} + v\frac{\partial\rho_{21}(z, t, v)}{\partial z} = -i\omega_{FF'}\rho_{21}(z, t, v) + iC_{FF'}\frac{dE(z, t)}{\hbar} - \frac{\Gamma_t}{2}\rho_{21}(z, t, v). \quad (2)$$

Taking the Fourier transform of this equation with respect to t and z , in the quasi-resonant approximation, we obtain:

$$\rho_{21}(k, \omega, v) = iC_{FF'}\frac{dE(k, \omega)}{2\hbar} \frac{1}{\Gamma_t/2 - i(\Delta_{FF'} - kv)}, \quad (3)$$

with $\Delta_{FF'} = \omega - \omega_{FF'}$. In the (k, ω) space and for an *homogeneous medium*, the relation between the polarization and the field is: $P(k, \omega, v) = \epsilon_0\chi(k, \omega, v)E(k, \omega)$. Furthermore, in the dilute approximation, $P(k, \omega, v) = 2N d C_{FF'} M_v(v)\rho_{21}(k, \omega, v)$, with N the density of the vapor and $M_v(v)$ the Maxwell Boltzman velocity distribution. Consequently the susceptibility of the vapour in the (k, ω) space is:

$$\chi(k, \omega, v) = iNM_v(v)\frac{C_{FF'}^2 d^2}{\hbar\epsilon_0} \frac{1}{\Gamma_t/2 - i(\Delta_{FF'} - kv)}. \quad (4)$$

This susceptibility depends explicitly on k through the Doppler shift, and this is the reason for the non-local response of the medium (i.e. the spatial dispersion). We note that this approach using a convective derivative is similar to the one used to derive the permittivity of a metal in the anomalous skin-depth situation [3]. The inverse Fourier transform in k yields the susceptibility:

$$\chi(z - z', \omega, v) = iNM_v(v)\frac{C_{FF'}^2 d^2}{\hbar\epsilon_0} \frac{1}{2\pi} \int_{-\infty}^{\infty} \frac{e^{ik(z-z')}}{\Gamma_t/2 - i(\Delta_{FF'} - kv)} dk. \quad (5)$$

To calculate the integral, we integrate in the k -complex plane. When applying the residue theorem, care must be taken, as the position of the pole $k_0 = (\Delta_{FF'} + i\Gamma_t/2)/v$ in the plane depends on the sign of the velocity. We obtain the non-local response function presented in the main text [Eq.(5)]:

$$\chi(z - z', \omega, v) = 0 \quad \text{when} \quad \frac{z - z'}{v} < 0, \quad (6)$$

$$\chi(z - z', \omega, v) = iNM_v(v)\frac{C_{FF'}^2 d^2}{\hbar\epsilon_0|v|} \exp\left[\left(-\frac{\Gamma_t}{2} + i\Delta_{FF'}\right)\frac{z - z'}{v}\right] \quad \text{when} \quad \frac{z - z'}{v} > 0. \quad (7)$$

The expression (7) shows that the distance ξ over which the polarization depends on the field (i.e. the range of non-locality) is $\xi = |v|/\Gamma_t$, thus confirming the qualitative discussion in the main text. Furthermore the fact that $\chi(z - z', \omega, v)$ depends on the sign of $(z - z')/v$ indicates that the optical response at position z only depends on atoms located at position $z' < z$ moving with a positive velocity and on atoms at $z' > z$ having a negative velocity.

B. Transmitted field for a dilute slab placed in vacuum

We first consider an atomic slab of thickness L placed in vacuum, i.e. we do not consider the sapphire windows of the nano-cell. The slab is excited by a plane wave (frequency ω) with complex amplitude $E_0 \exp[ik_1 z]$ where $k_1 = \omega/c$. Using the superposition principle, the amplitude of the field transmitted after the slab is [4, 5]:

$$E_t(z > L) = E_0 e^{ik_1 z} + \frac{ik_1}{2\epsilon_0} \int_0^L dz' P(z', \omega) e^{ik_1(z-z')} . \quad (8)$$

In a non-local linear medium consisting of atoms moving with velocity v (distribution $M_v(v)$) as considered here, the relation between the polarization vector and the field is:

$$P(z, \omega) = \int_{-\infty}^{\infty} dz' \int_{-\infty}^{\infty} dv \epsilon_0 \chi(z, z', \omega, v) E(z') , \quad (9)$$

leading to the following expression for the transmitted field:

$$E_t = E_0 e^{ik_1 z} + \frac{ik_1}{2\epsilon_0} \int_0^L dz' e^{ik_1(z-z')} \left[\int_{-\infty}^{\infty} dz'' \epsilon_0 \left(\int_{-\infty}^{\infty} dv \chi(z', z'', \omega, v) \right) E(z'') \right] . \quad (10)$$

The hypothesis of quenching collisions at the edge of the slab (second hypothesis at the beginning of Sec. IA) leads to a breaking of the translational invariance by the interfaces, a fact that we express by multiplying the susceptibility of (7) by a top-hat function ($\Pi_0^L(z') = 1$ for $0 < z' < L$ and is null elsewhere): $\chi_L(z', z'', \omega, v) = \chi(z' - z'', \omega, v) \Pi_0^L(z')$. Using the expression of the non-local susceptibility (7), the second term of (10) is a sum of two integrals:

$$I_0 = \frac{ik_1}{2\epsilon_0} \int_0^L dz' e^{ik_1(z-z')} \left[\int_0^{z'} dz'' \epsilon_0 \left(\int_0^{\infty} dv \frac{iNC_{FF'}^2 d^2}{\hbar\epsilon_0 v} e^{\frac{z'-z''}{v}(-\frac{\Gamma_t}{2} + i\Delta_{FF'})} M_v(v) \right) E(z'') \right] \quad (11)$$

$$I'_0 = \frac{ik_1}{2\epsilon_0} \int_0^L dz' e^{ik_1(z-z')} \left[\int_{z'}^L dz'' \epsilon_0 \left(\int_{-\infty}^0 dv \frac{-iNC_{FF'}^2 d^2}{\hbar\epsilon_0 v} e^{\frac{z'-z''}{v}(-\frac{\Gamma_t}{2} + i\Delta_{FF'})} M_v(v) \right) E(z'') \right] . \quad (12)$$

The separation of the integral in Eq. (10) into two integrals, one involving negative velocities, and the other positive ones, using Eqs. (6) and (7) for $\chi(z' - z'', \omega, v)$ also comes from the assumptions that the atoms lose their coherence at the boundaries of the slab. Otherwise, an atom with a velocity $-v$ would bounce off the surface, switching its velocity to $+v$, and would contribute to the polarization even for $z' < z$.

In order to proceed further, we need the expression of the field inside the vapor. As we consider a dilute atomic medium placed in vacuum, we neglect the reflection at the boundaries of the slab and take $E(z'') \approx E_0 \exp[ik_1 z'']$. The integrals I_0 and I'_0 become respectively:

$$I_0 = -\frac{NC_{FF'}^2 d^2}{2\hbar\epsilon_0} E_0 \exp[ik_1 z] \int_0^{\infty} dv M_v(v) \left(\frac{k_1 L}{\Lambda} + \frac{k_1 v e^{-\frac{\Lambda L}{v}}}{\Lambda^2} - \frac{k_1 v}{\Lambda^2} \right) , \quad (13)$$

$$I'_0 = -\frac{NC_{FF'}^2 d^2}{2\hbar\epsilon_0} E_0 \exp[ik_1 z] \int_{-\infty}^0 dv M_v(v) \left(\frac{k_1 L}{\Lambda} - \frac{k_1 v e^{\frac{\Lambda L}{v}}}{\Lambda^2} + \frac{k_1 v}{\Lambda^2} \right) , \quad (14)$$

where we have introduced, as in Ref. [6], $\Lambda = \Gamma_t/2 - i(\Delta_{FF'} - k_1 v)$. Combining Eqs.(10), (13) and (14), the final expression of the field transmitted after the slab is:

$$E_t = E_0 e^{ik_1 z} \left[1 - \frac{NC_{FF'}^2 d^2}{2\hbar\epsilon_0} \int_{-\infty}^{\infty} dv M_v(v) \left(\frac{k_1 L}{\Lambda} - \frac{k_1 |v|}{\Lambda^2} + \frac{k_1 |v| e^{-\frac{\Lambda L}{|v|}}}{\Lambda^2} \right) \right] , \quad (15)$$

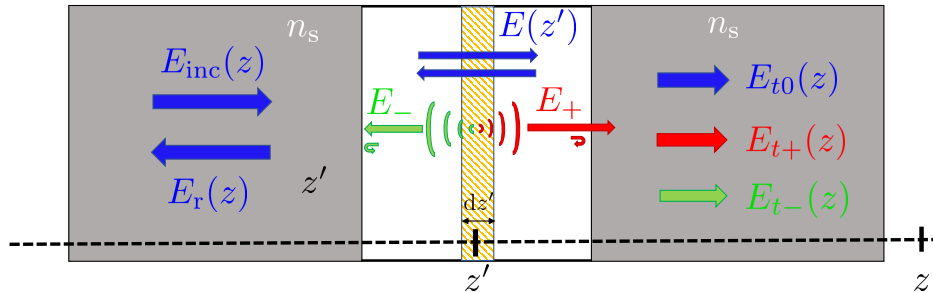


FIG. 1: Configuration used to calculate the transmission through the cell. The dilute vapour is confined between two sapphire plate of index n_s . The incident field $E_0 \exp[ik_1 z]$ undergoes multiple reflections inside the cell before being finally transmitted (E_{t0}). The field $E(z')$ inside the cell excite the atoms in the slice dz' , and radiate a field in the forward (backward) direction E_+ (E_-) that is reflected multiple times before leading to the transmitted fields E_{t+} (E_{t-}).

Equation (15) is equivalent to the one derived by several authors [6, 7] starting from a different point of view, which made the non-locality less explicit than the above derivation. We now discuss the contributions of the three integrals (labeled J_1 , J_2 and J_3 respectively) in Eq. (15) (see also [6]).

1. The first term J_1 is the one we would have obtained had we simply taken for the susceptibility $\chi(z, z', \omega, v)$ of atoms at velocity v the local, Doppler-shifted (and incorrect!) expression:

$$\chi(z - z', \omega, v) = i \frac{NC_{FF'}^2 d^2}{\hbar \epsilon_0} \frac{M_v(v)}{\Gamma_t/2 - i(\Delta_{FF'} - k_1 v)} \delta(z - z') \quad (16)$$

where the detuning $\Delta_{FF'} = \omega - \omega_{FF'}$. Although intuitive, this approach would have missed the contributions from the two remaining terms, which are important in the mesoscopic regime. The term J_1 dominates as soon as $L \gtrsim |v/\Lambda|$. Close to resonance and for $kv \lesssim \Gamma_t$, this yields $L \gtrsim \xi$. This indicates that in large cells ($L \gtrsim 1 \mu\text{m}$), J_1 is the dominant contribution and the conventional dispersion theory applies.

2. The second and third terms J_2 and J_3 become important as soon as $|v|/(|\Lambda|L) \gtrsim 1$, i.e. $L \lesssim \xi$. These two terms are specific to the mesoscopic regime and are a consequence of the non-local character of the atomic response. They dominate for thin cells.
3. Finally, the third term $J_3 \sim J_2 \exp[-L/\xi]$ describes the fact that the atomic dipole stops emitting when it reaches the boundary of the slab. When $J_2 \gtrsim J_1$, we have seen that $L < \xi$ and $J_3 \sim J_2$, indicating that in the mesoscopic regime it is not possible that J_2 alone dominates.

C. Transmitted field in a dilute regime with cavity boundaries

We now consider the more involved case where the atomic slab is confined between the two windows of the cell (index n_s), leading to a pronounced cavity effect. This situation has already been discussed, in particular in Ref. [8] starting

from a different point of view. Here we use the non-local susceptibility given by Eq.(7) to derive the transmission of the slab confined in the nanocell.

Figure 1 summarizes the different fields involved. First, we need to consider the field inside the empty cavity between the two windows, which reads:

$$E(z'') = \frac{E_0 t_1}{1 - r_2^2 e^{2ik_1 L}} \left(e^{ik_1 z''} + r_2 e^{ik_1(2L - z'')} \right) \quad (17)$$

with $t_1 = 2n_s/(1 + n_s)$ and $r_2 = (1 - n_s)/(1 + n_s)$. Second, the field emitted by the atoms of the vapor also undergoes multiple reflections on the cavity walls. We separate this field into two components propagating respectively in the forward and backward directions and consider the multiple reflections of each. Consequently, the field transmitted after the cell results from the interference of (i) the field $E_{t0} = \frac{t_1 t_2}{1 - r_2^2 e^{2ik_1 L}} E_0 e^{ik_1 z}$ of the cavity without any atoms, (ii) the field E_{t+} emitted by all slices dz' initially directed in the forward direction and undergoing multiple reflections, and (iii) the field E_{t-} initially emitted in the backward direction, also undergoing reflections. The transmitted field is therefore:

$$E_t(z) = \frac{t_1 t_2}{1 - r_2^2 e^{2ik_1 L}} E_0 e^{ik_1 z} + E_{t+}(z) + E_{t-}(z), \quad (18)$$

with $t_2 = 2/(n_s + 1)$. The field emitted by the atoms in the forward direction is, taking into account the non-local relation between $P(z)$ and $E(z)$ inside the vapor:

$$E_{t+} = A \frac{ik_1}{2\epsilon_0} \int_0^L dz' e^{ik_1(z-z')} \left[\int_{-\infty}^{\infty} dz'' \epsilon_0 \left(\int_{-\infty}^{\infty} dv \chi_L(z', z'', \omega, v) \right) E(z'') \right] \quad (19)$$

with

$$A = t_2(1 + r_2^2 e^{2ik_1 L} + r_2^4 e^{4ik_1 L} + \dots) = \frac{t_2}{1 - r_2^2 e^{2ik_1 L}} \quad (20)$$

the prefactor that accounts for the multiple reflections before the field exits the cavity. To calculate the integral we again assume a dilute vapor and use the expression (17) valid for an empty cavity. Calculations similar to the ones performed for the slab immersed in vacuum (Sec.IB) lead to:

$$E_{t+} = ABC (I_1 + I_2) E_0 \exp[ik_1 z] \quad (21)$$

with

$$I_1 = - \int_0^{\infty} dv M_v(v) \left[\frac{L}{\Lambda_+} + \frac{v}{\Lambda_+^2} e^{-\Lambda_+ \frac{L}{v}} - \frac{v}{\Lambda_+^2} + \frac{r_2 e^{2ik_1 L}}{\Lambda_-} \left(\frac{1}{2ik_1} (1 - e^{-2ik_1 L}) + \frac{v}{\Lambda_+} (e^{-\Lambda_+ \frac{L}{v}} - 1) \right) \right], \quad (22)$$

and

$$I_2 = \int_{-\infty}^0 dv M_v(v) \left[- \frac{L}{\Lambda_+} + \frac{v}{\Lambda_+^2} e^{\Lambda_+ \frac{L}{v}} - \frac{v}{\Lambda_+^2} + \frac{r_2 e^{2ik_1 L}}{\Lambda_-} \left(\frac{1}{2ik_1} (e^{-2ik_1 L} - 1) + \frac{v}{\Lambda_+} e^{\Lambda_- \frac{L}{v}} (1 - e^{-\Lambda_+ \frac{L}{v}}) \right) \right], \quad (23)$$

where we have introduced $\Lambda_{\pm} = \Gamma_t/2 - i(\Delta_{FF'} \mp k_1 v)$, $B = t_1/(1 - r_2^2 e^{2ik_1 L})$ and $C = NC_{FF'}^2 d^2 k_1/(2\hbar\epsilon_0)$.

We proceed in a similar way for the field E_{t-} initially emitted in the backward direction, noting that the polarization vector at position z' due to the backward emitted field is retarded by a factor $r_2 e^{2ik_1 z'}$ (see Fig. 1). We get:

$$E_{t-} = Ar_2 \frac{ik_1}{2\epsilon_0} \int_0^L dz' e^{ik_1(z+z')} \left[\int_{-\infty}^{\infty} dz'' \epsilon_0 \left(\int_{-\infty}^{\infty} dv \chi_L(z', z'', \omega, v) \right) E(z'') \right]. \quad (24)$$

This leads to:

$$E_{t-} = r_2 ABC(I_3 + I_4)E_0 \exp[ik_1 z] \quad (25)$$

with

$$I_3 = - \int_0^\infty dv M_v(v) \left[\frac{1}{\Lambda_+} \left(\frac{e^{2ik_1 L} - 1}{2ik_1} + \frac{v}{\Lambda_-} (e^{-\Lambda - \frac{L}{v}} - 1) \right) + \frac{r_2 e^{2ik_1 L}}{\Lambda_-} \left(L + \frac{v}{\Lambda_-} (e^{-\Lambda - \frac{L}{v}} - 1) \right) \right] \quad (26)$$

and

$$I_4 = \int_{-\infty}^0 dv M_v(v) \left[\frac{1}{\Lambda_+} \left(\frac{1 - e^{2ik_1 L}}{2ik_1} + \frac{v}{\Lambda_-} (e^{\Lambda + \frac{L}{v}} - e^{2ik_1 L}) \right) + \frac{r_2 e^{2ik_1 L}}{\Lambda_-} \left(-L + \frac{v}{\Lambda_-} (e^{\Lambda - \frac{L}{v}} - 1) \right) \right]. \quad (27)$$

Finally, the transmitted field is:

$$E_t(z) = \left(\frac{t_1 t_2}{1 - r_2^2 e^{2ik_1 L}} + ABC [I_1 + I_2 + r_2(I_3 + I_4)] \right) E_0 \exp[ik_1 z]. \quad (28)$$

We retrieve the expression obtained in Ref. [8] using a different approach. Here again, the fact that in Eqs. (19) and (24) we can separate the integral into two integrals involving only the positive [Eqs.(22) and (26)] or the negative velocities [Eqs.(23) and (27)] comes from the assumptions that the atomic coherences are lost in a quenching collisions at the cell walls.

D. Case of a multilevel atom

So far we have considered a single atomic transition. In the experiment, several hyperfine transitions of the D1 cesium line contribute. In order to account for them we calculate the susceptibility by summing over all transitions and Eqs. (15) and (28) respectively become:

$$E_t = E_0 e^{ik_1 z} \left[1 - \sum_{FF'} \frac{NC_{FF'}^2 d^2}{4\hbar\epsilon_0} \int_{-\infty}^\infty dv M_v(v) \left(\frac{k_1 L}{\Lambda} - \frac{k_1 |v|}{\Lambda^2} + \frac{k_1 |v| e^{-\frac{\Lambda L}{|v|}}}{\Lambda^2} \right) \right], \quad (29)$$

$$E_t(z) = \left(\frac{t_1 t_2}{1 - r_2^2 e^{2ik_1 L}} + \sum_{FF'} ABC [I_1 + I_2 + r_2(I_3 + I_4)] \right) E_0 \exp[ik_1 z], \quad (30)$$

where the detuning appearing in Λ is $\Delta_{FF'} = \omega - \omega_{FF'}$.

II. BIMODAL VELOCITY DISTRIBUTION

At the end of the main text, we compare two models: a phenomenological model where we use the local susceptibility, but modify the velocity distribution to account for the non locality due to the interface, taking $M_v(v) = \delta(v)$, and the more accurate non-local model derived in Sec.I. We conclude that the second non-local model is able to explain the data in a more satisfactory way, as it yields a linewidth Γ_p independent of L . We show here that the use of a more refined velocity distribution in phenomenological model does not affect this conclusion.

To do so, we use a bimodal normalized velocity distribution, already introduced in the context of nano-cells [9]:

$$M_v(v) = W \left(a \exp \left[-\frac{v^2}{u^2} \right] + (1 - a) \exp \left[-\left(\frac{v}{su} \right)^2 \right] \right), \quad (31)$$

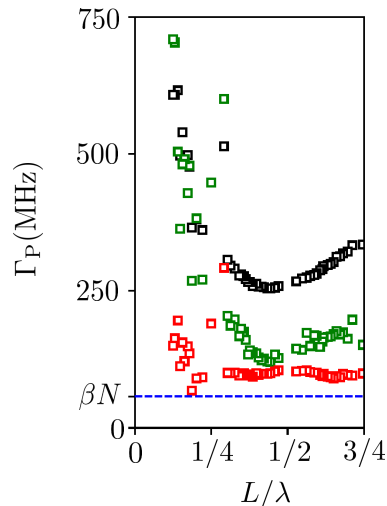


FIG. 2: Fitted broadening parameter Γ_p versus the cell thickness L . Black squares: phenomenological model where we use the local susceptibility with $M_v(v) = \delta(v)$. Green squares: same using the bimodal velocity distribution. Red squares: accurate non-local model as derived in Sec. I.

where $u = \sqrt{2k_B T/M}$ is the root-mean square velocity and $W = (au\sqrt{\pi} + (1-a)su\sqrt{\pi})^{-1}$. The additional parameters a and s describe respectively the fraction of slow atoms and the width of the component of the distribution corresponding to the fast atoms. This bimodal distribution therefore consists in a pedestal associated to the slow atoms and a sharp feature superimposed on coming from the fast atoms. We fit the data using this velocity distribution in the local model with N , Γ_p , Δ_p , a and s as free parameters. The result is shown in Fig. 2 as green squares. Similarly to the case where $M_v(v) = \delta(v)$, the strong dependence of Γ_p with L is not compatible with a physical interpretation.

III. DEVIATION FROM BEER-LAMBERT TRANSMISSION LAW

Figures 3(a,b) of the main text show that the minimum of transmission of the hyperfine transition $F = 4$ to $F' = 3$ does not follow the Beer-Lambert law. To gain further insight on this behavior, we study the evolution of the minimum of the theoretical transmission T_{\min} as a function of the vapor thickness L . To separate the effect of the cavity from the one of the non-local response, we consider two models: (i) the first local model of the text that accounts for the cavity (Eq. (3) of main text) with a local index of refraction. (ii) the non-local model, but without the cavity surrounding the atomic (Eq. (18) of the Supplemental Material). The results are shown in Fig. 3. We observe that the cavity surrounding a local-medium leads to an oscillation of T_{\min} with L with a period $\lambda/2$, as it should for a standing wave in a cavity. The non-local response of the cloud results into an oscillation of T_{\min} with a period λ . This can also be seen from Eq. (15) where the last term $\exp[-\Lambda L/|v|]$ leads to an oscillatory dependence in $k_1 L$.

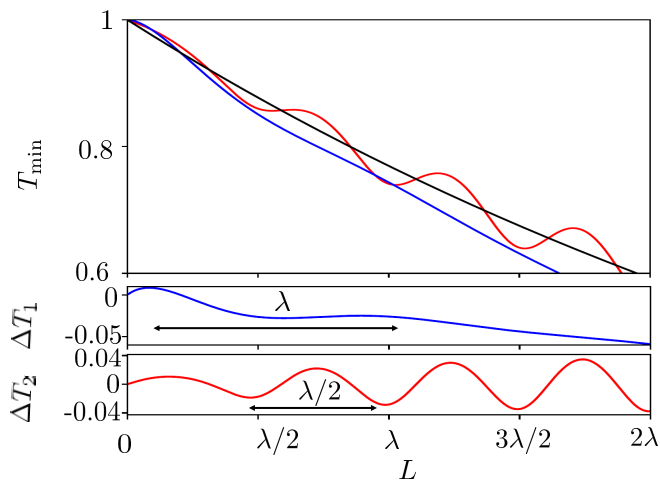


FIG. 3: Top : Minimum of the transmission, T_{\min} , versus L extracted from the local model including the cavity (red line) and from the non-local model without any cavity surrounding the slab (blue line). Black line : prediction of the Beer-Lambert law. Parameters used : $\Delta_p = 0$, $\Gamma_p = 2\pi \times 100$ MHz and $\Theta = 188^\circ\text{C}$. Bottom : deviations of the non-local (ΔT_1) and local (ΔT_2) models from the Beer Lambert law.

IV. THICKNESS DEPENDENCE OF Γ_p IN THE PHENOMENOLOGICAL SECOND MODEL

In Fig.3(c) of the main text, we observe a strong dependence of the broadening parameter Γ_p with the thickness L for the phenomenological model. In this section we deconvolve the effects of the Casimir atom-surface interaction from the non-local influence of the surface when $\xi \geq L$ on the parameter Γ_p returned by the fit. To understand the sharp increase for small L , we simulate a collection of spectra with the accurate non-local model of Sec. I for a fixed temperature ($\Theta = 170^\circ\text{C}$), a fixed broadening $\Gamma_p = 100$ MHz and various L between $\lambda/8$ and $3\lambda/4$. We do not include the Casimir atom-surface interaction in the model. We then fit each generated spectra by the *phenomenological* model and extract the corresponding Γ_p . The result is shown as a violet dashed line in Fig. 4.

We observe a very good agreement of the fitted Γ_p for the experimental and simulated data using the accurate non-local model for $L \gtrsim 150$ nm. This indicates that the increase of Γ_p at small L is a feature of the phenomenological, non-local model. The sharper increase for $L \leq 150$ nm is therefore ascribed to the Casimir atom-surface interactions, and can also be seen in the variation of Γ_p returned by the accurate non-local model with L .

-
- [1] M.F.H. Schuurmans, Spectral narrowing of selective reflection, *Journal de Physique* **37**, 469 (1976).
 - [2] G. Grynberg, A. Aspect and C. Fabre, Introduction to Quantum Optics, Cambridge University Press, New York (2010).
 - [3] P.W. Gilbert, The anomalous skin effect and the optical properties of metals, *J. Phys. F* **12**, 1845 (1982).
 - [4] H. Fearn, D.F.V. James and P. Milonni, Microscopic approach to reflection, transmission and the Ewald-Osen extinction theorem, *Am. J. Phys.* **64**, 986 (1996).
 - [5] R.P. Feynman, R.B. Leighton and M. Sands, *Lectures on Physics*, vol. 1, chap. 30, Addison Wesley (2006).
 - [6] S. Briaudeau *et. al.*, Coherent Doppler narrowing in a thin vapor cell: Observation of the Dicke regime in the optical domain, *Phys. Rev. A* **57**, 5 (1998).

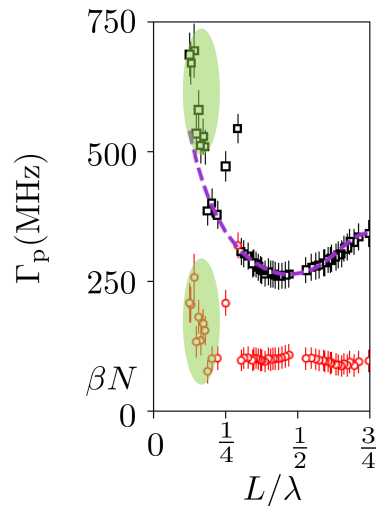


FIG. 4: Broadening parameter Γ_p obtained from the fit of the experimental spectra using the *phenomenological* second model of the main text (black squares) and the non-local model of Sec. I (red circles). Error bars are the quadratic sum of statistic and fit errors. The violet dashed line is the broadening parameter Γ_p obtained from the fit using the phenomenological non-local model of the data simulated by the expression derived in Sec. IC. Green shaded areas indicate the region where the Casimir atom-surface interactions dominate the broadening.

- [7] T.A. Vartanyan and D.L. Lin, Enhanced selective reflection from a thin layer of a dilute gaseous medium, *Phys. Rev. A* **51**, 1959 (1995).
- [8] G. Dutier and M. Ducloy, Revisiting optical spectroscopy in a thin vapor cell: mixing of reflection and transmission as a Fabry Perot microcavity effect, *J. Opt. Soc. Am. B* **20**, 793 (2003).
- [9] K.A. Whittaker, J. Keaveney, I.G. Hughes, A. Sargsyan, D. Sarkisyan, and C.S. Adams, Spectroscopic detection of atom-surface interactions in an atomic-vapor layer with nanoscale thickness, *Phys. Rev. A* **92**, 052706 (2015).